

2. LITERATURE REVIEW

2.1 Electrodeposition

Electrodeposition or electroplating is a form of metal finishing. It is often regarded as both an art and a science because its theory and practices are derived from many branches of science and technology. Electroplating is a branch of electrochemistry which uses electrical energy to deposit a metal coating onto a conducting substrate in order to impart much improved physical properties such as:

1. Resistance to wear
2. Increased electrical conductivity, for example in printed circuit boards,
3. Increased magnetic susceptibility, for example on printed circuit boards,
4. Increased surface reflectivity, for example for decorative purposes.

Electrodeposition occurs during electrolysis in a solution known as “electrolyte”. The current enters and leaves the electrolyte via two conducting electrodes which are called the “anode” and “cathode”. The overall (conventional) current flow and the principle components of an electroplating process are shown schematically in **Figure 2.1** [10].

1. An electroplating bath containing a conducting salt and the metal to be plated in a soluble form. , as well as perhaps additives.
2. The electronically conducting cathode, i.e. the work piece to be plated.
3. The anode (also electronically conducting) preferably insoluble.
4. An inert vessel to contain (1)-(3), typically, e.g. polypropylene, polyvinylchloride.

5. A d.c. electrical power source, usually a regulated transformer/ rectifier. (**Figure 2.2)**)

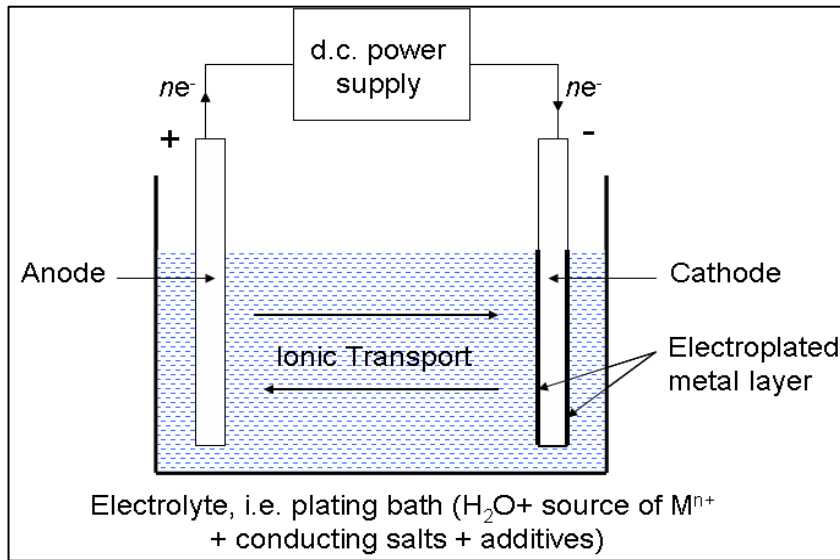
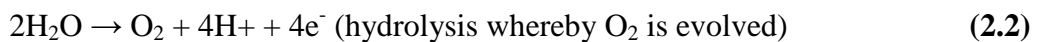


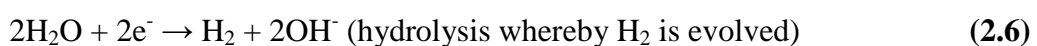
Figure 2.1: Schematic diagram showing an electroplating process

During electrolysis, all the ions in solution carry current and the current capacity depends on its concentration and mobility at the electrodes. Eventually this leads to a build-up (i.e. an excess) of positive ions or cations at the cathode, and those with most positive discharge potentials are first reduced. The anions with most negative discharge potential are oxidized at the anode. At each electrode, there are more than one reactions occurring.

At the anode:



At the cathode:





If the metal deposition process is the major process, it is said to have good current efficiency [11].

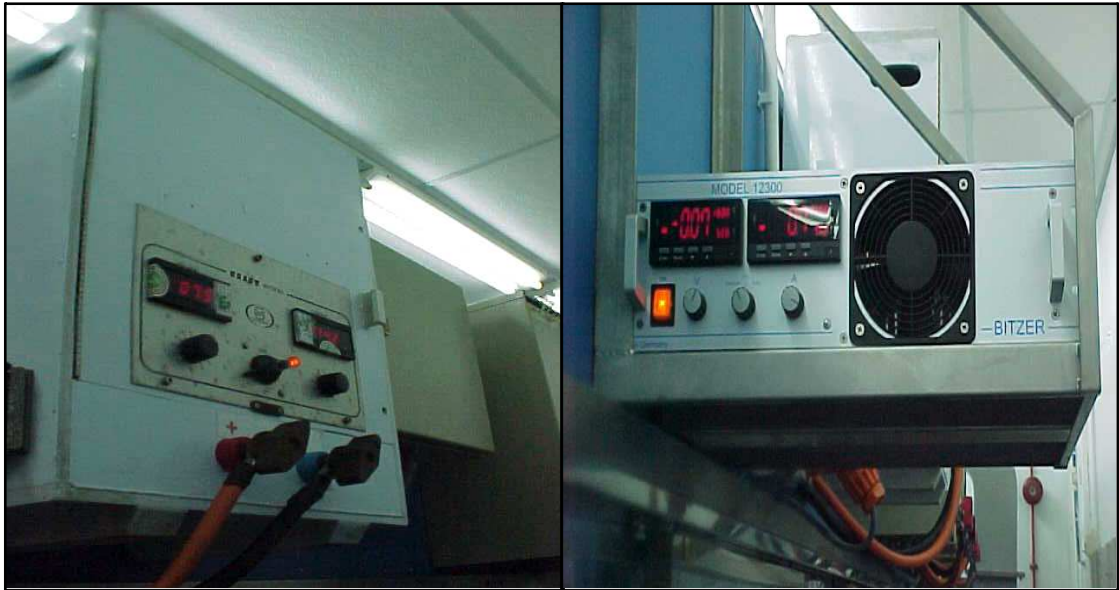


Figure 2.2: A d.c. rectifier used in electroplating industry

2.2 Electroplating mechanism

If a voltage is applied across the two electrodes in an electrolysis cell, a current consisting of electron flow, will be set up, with these moving from the anode, through the external circuit and back to the cathode. The anode will thereby dissolve anodically, and the cations so formed will migrate to the cathode. Anions present in solution will move in the opposite direction towards the anode. Current will thus flow through the solution by virtue of the movement of these charged ions and this is known as ionic current, or electrolytic conductance. Of critical importance in electrodeposition, is the mechanism by which metal cations are delivered to the cathode, and the means for their replenishment as they are lost to solution by deposition at the cathode. The rate at which fresh ions (and also uncharged species required for reaction) are delivered to the cathode surface from the bulk of solution, depends on the prevailing hydrodynamic

conditions at and near the cathode surface. There are three main mechanisms involved in delivery of ions to the electrode surface, these being [12]:

1. Migration (under a potential gradient),
2. Diffusion (under a concentration gradient)
3. Convection (movement of the electrolyte liquid itself).

2.2.1 Migration

Voltage applied across the electrodes of an electrolysis cell sets up an electrical field between anode and cathode. Assuming that the electrolytic conductivity of the electrolyte is the same at all points in solution, the potential gradient is given by the voltage across the solution (excluding overvoltage at the electrodes) divided by the distance between the electrodes. The magnitude of this potential gradient determines the rate at which ions move through solution. The term 'migration' is understood here as the movement of charged species in solution under a potential gradient. The effect operates throughout the solution, anions being electrostatically attracted to the anode, cations to the cathode. The progress of such ions through solution is impeded by collisions with solvent molecules and viscous drag as the ions, with their hydration sheaths, move through the liquid. The ions thereby acquire a given velocity, depending on the nature of the ion, the potential gradient, solution viscosity, etc. These velocities are very low, of the order of micrometers per second. It follows that the overall contribution to the supply of ions resulting from the migration process is very small, and can generally be neglected [12,13].

2.2.2 Convection

In contrast to the preceding and following transport mechanisms which involve the movement of species through an electrolyte, convection can be said to be the movement of reactants, etc. with the electrolyte. The so-called 'convective mass transport' results from movement of the bulk solution, whether by stirring, movement of the work through the solution (deliberate measures to enhance convection, known as 'forced convection') or by the natural circulation of a liquid caused by adventitious differences in solution density caused by thermal effects. Such movement of solution ceases to be significant in the region immediately adjacent to the electrode surface, where a liquid layer sometimes known as the 'stagnant layer' or more usually as the 'diffuse layer' is formed. Movement of ions etc across this diffuse layer takes place by diffusion. Convection is important not only because it moves the solution (with dissolved species) up to the diffuse layer, but also because the thickness of the diffuse layer is determined by convective action. The stronger the agitation (pumping, stirring, air-purging) the thinner is the diffuse layer [12,14].

2.2.3 Diffusion

The penultimate step, before charge transfer takes place at the electrode surface, is the migration of species, both charged and uncharged, across the diffuse layer. The driving force here is the concentration gradient, more formally expressed as chemical potential. The concentration of species at the electrode surface will, under open circuit conditions, be much the same as that in bulk solution. However, once current flows, species will, by their reaction, be removed at the electrode surface and a concentration gradient will be established. The tendency of species to move from regions of high concentration to

those of lower concentration, are what drive the diffusion process, and this is enshrined in Fick's laws of diffusion. The thickness of the 'diffuse layer', also known as the Nernst or Nernstian layer, is denoted by δ . Without forced convection, in a static solution, δ would be approximately 0.2 mm. Under conditions of forced convection, this value will decrease, and can reach values as low as 0.001 mm. It is generally assumed that diffusion is the only significant transport mechanism operating within the Nernstian layer. **Figure 2.3** shows what might be described as a concentration-depth profile. It shows the electrode surface as a vertical line on the left of the diagram. The vertical dashed line indicates the outer edge of the Nernst layer. The solid line shows the concentration profile predicted by the Nernst equation, the curved dashed line shows typical experimental results.

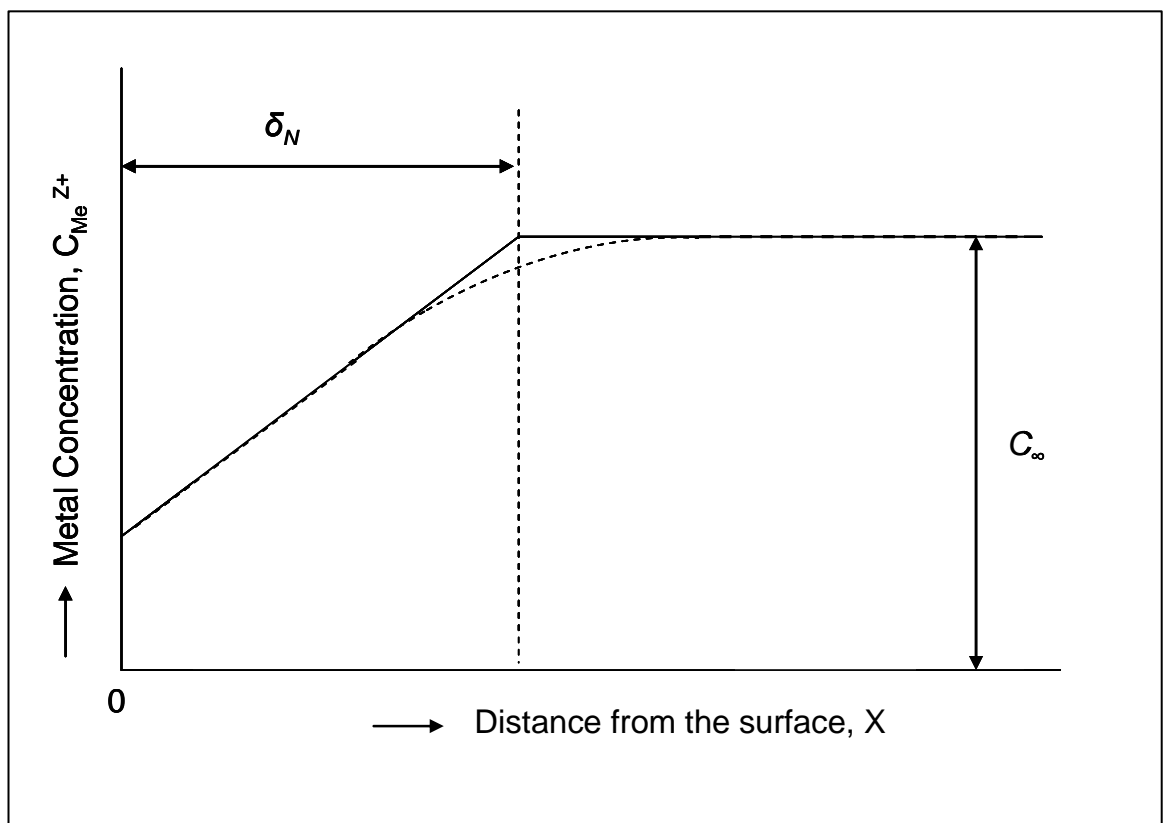


Figure 2.3: Metal ion concentration profile as a function of distance from the surface

Figure 2.3 depicts the situation in a typical electrolysis and shows how the concentration of reactants is depleted at the electrode surface. In the extreme case, the

concentration of reactants at the electrode surface is zero. Otherwise expressed, the species arriving at the electrode surface react instantly. The flux of cations through the diffuse layer, expressed as mol/s/cm² is known as the diffusion current density n^* . It is a function, as Fick's law indicates, of the concentration gradient across the Nernst layer, as expressed in **Equation 2.8**, where D is the diffusion coefficient, C_∞ is the metal ion concentration in bulk solution, C_c is the concentration at the electrode surface [12]:

$$n^* = D \frac{dc}{dx} = D \frac{(C_\infty - C_c)}{\delta_N} \quad (2.8)$$

At 100% cathode efficiency, the cathode current density i_c (A/cm²) is given by the following expression:

$$i_c = z * F * D \frac{(C_\infty - C_c)}{\delta_N} \quad (2.9)$$

where z is the number of electrons per ion being transferred, F the Faraday constant (96,485 C/equivalent). The cathodic current density is proportional to the value of $(C_\infty - C_c)/\delta_N$, the Nernstian concentration gradient. The metal ion concentration decreases from outside to inside of the Nernstian layer. If the current density is further increased, there comes a point where $C_c = 0$. The current is then said to have reached the diffusion-limited current density, or mass-transport-limited current density. Increasing the voltage, at this point, will then (on this simplified theory) bring no further increase in current. We can then rewrite **Equation 2.9** in a simplified form as below, **Equation 2.10** [15]:

$$i_D = z * F * D \frac{C_\infty}{\delta_N} \quad (2.10)$$

The rate of metal deposition is then limited to this value, mass-transport being the rate-determining step. The diffusion-limiting current density i_D represents the maximum

current density at which the metal can be deposited under the given hydrodynamic conditions. In practice, metals deposited under these conditions tend to be powdery or friable and of no practical use except where there is a deliberate intention to produce metal powders. Having crossed the Nernst diffusion layer, the metal ions face a further barrier separating them from the electrode surface, namely the electrode double layer or interfacial layer. This is formed, as indicated earlier, by the aggregation of electrons on one side of the interface, and metal ions on the other. As a first approximation, as shown in **Figure 2.4**, this can be modeled as an electrolytic capacitor. In this scheme, $\Delta\phi$ is the difference between the potential of the metal electrode, ϕ_{Me} and that of the solution, ϕ_L [12].

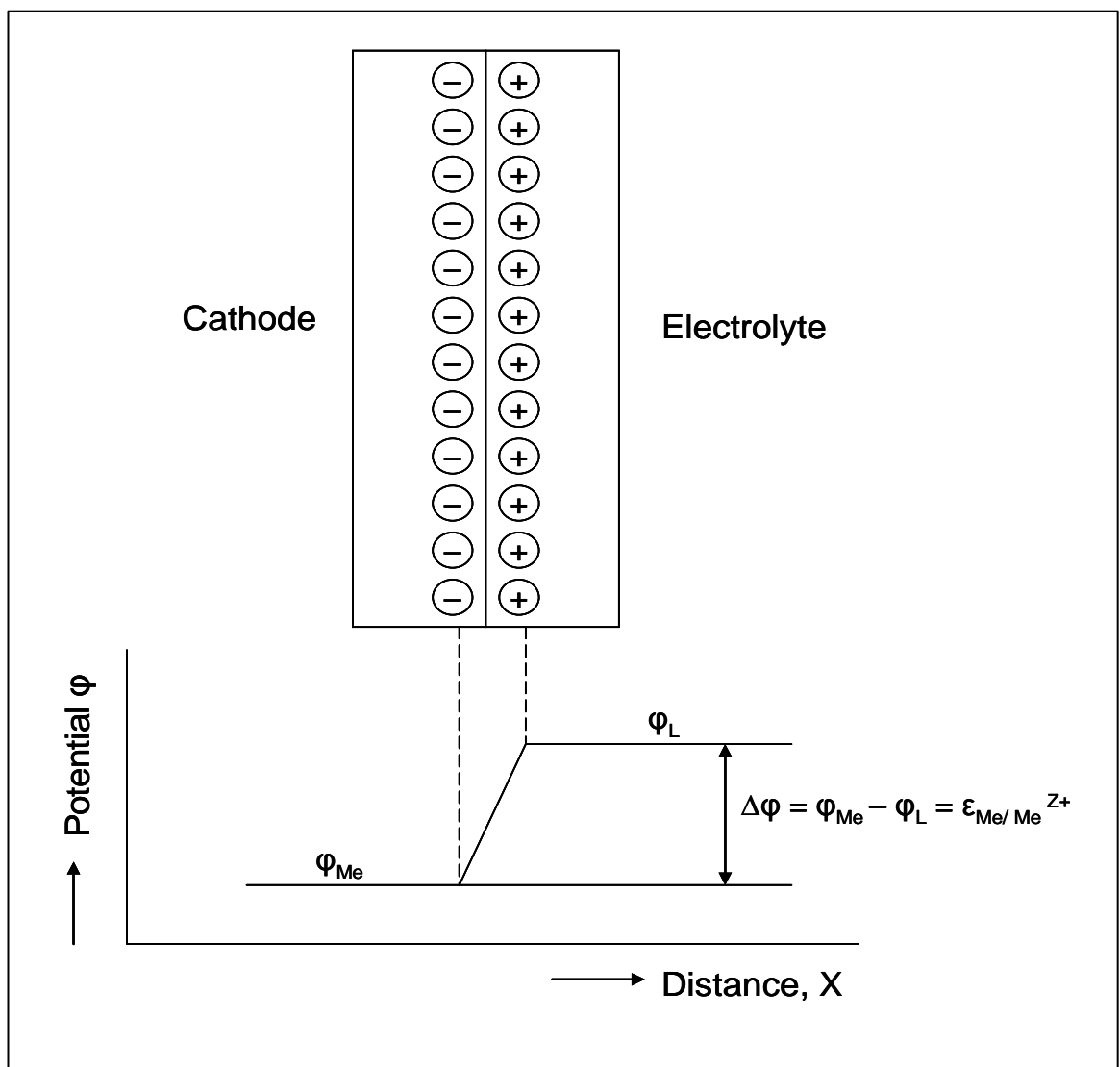


Figure 2.4: Structure of the electrical double layer at a metal-solution interface

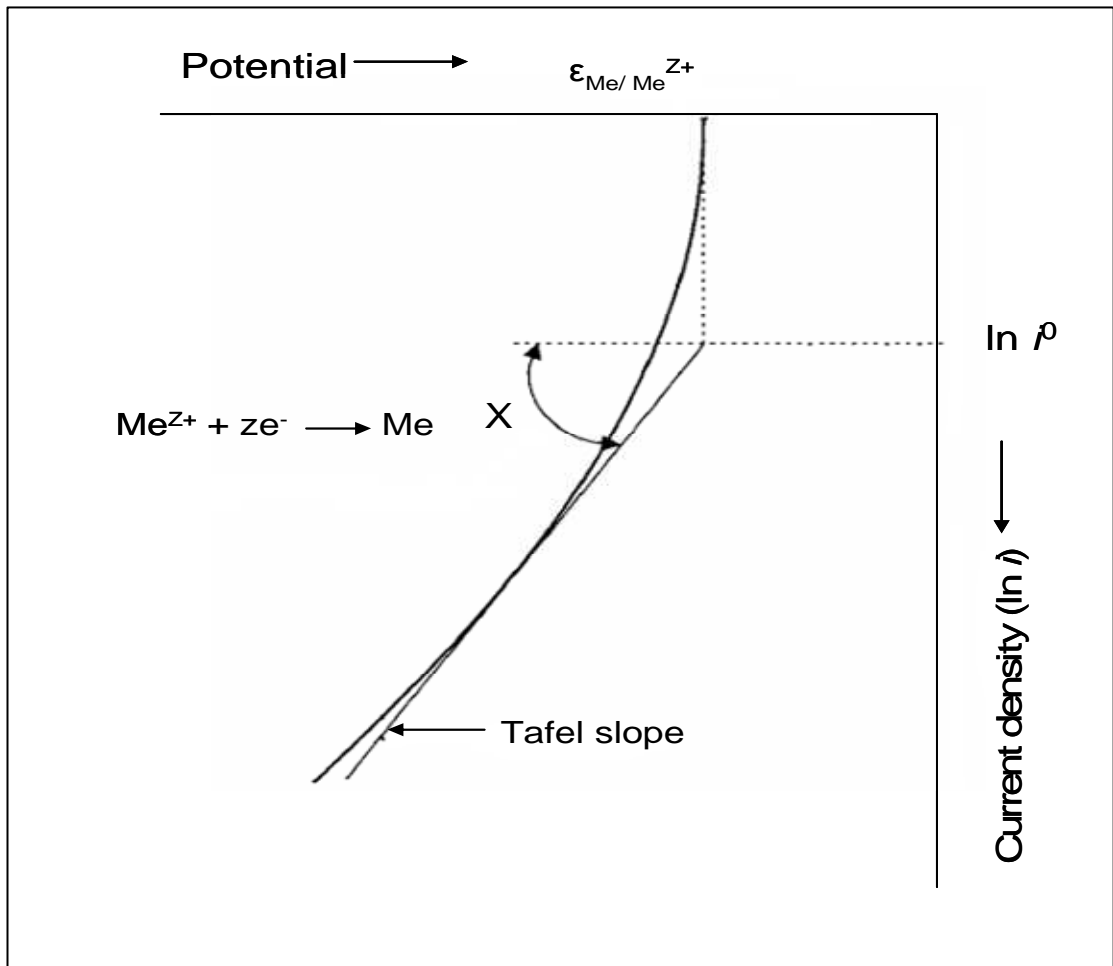


Figure 2.5: Dependence of cathodic current density on potential. Graphical determination of $\epsilon_{\text{Me}/\text{Me}^{Z+}}$, i^0 , and α by drawing a tangent to the curve

In **Figure 2.5**, the natural logarithm of the cathodic current density is plotted versus potential. As this representation shows, the value of the equilibrium potential can be derived from the asymptotic value of the log function. The corresponding exchange current density is derived by drawing a tangent and is given by the intersection of the tangent with the asymptotic value of the current-potential plot. This value, which is proportional to the transfer coefficient, is known as the Tafel slope, named after the German scientist who first derived an empirical relationship linking current density and overpotential. Cathodic deposition of metals is initiated by discharge of metal ions which are already in close proximity to the electrode. Thus, at the onset of the process, the rate determining step is the movement of the charged species through the electrical double layer to the electrode surface. This leads to a depletion of the dischargeable

metal ions in the near-electrode region, and metal electrodeposition can only continue if these are replenished from bulk solution. It follows that, in most cases (except at very low current densities and high metal ion concentrations), the deposition process is increasingly mass-transport controlled. In the limiting case, where mass transport becomes the rate controlling stage, the current-potential plot assumes the form seen in **Figure 2.6**. In practice, it must be recognized that only certain metals can be electrodeposited from aqueous solution and these are shown in **Figure 2.7** enclosed within the frame [12,16,17].

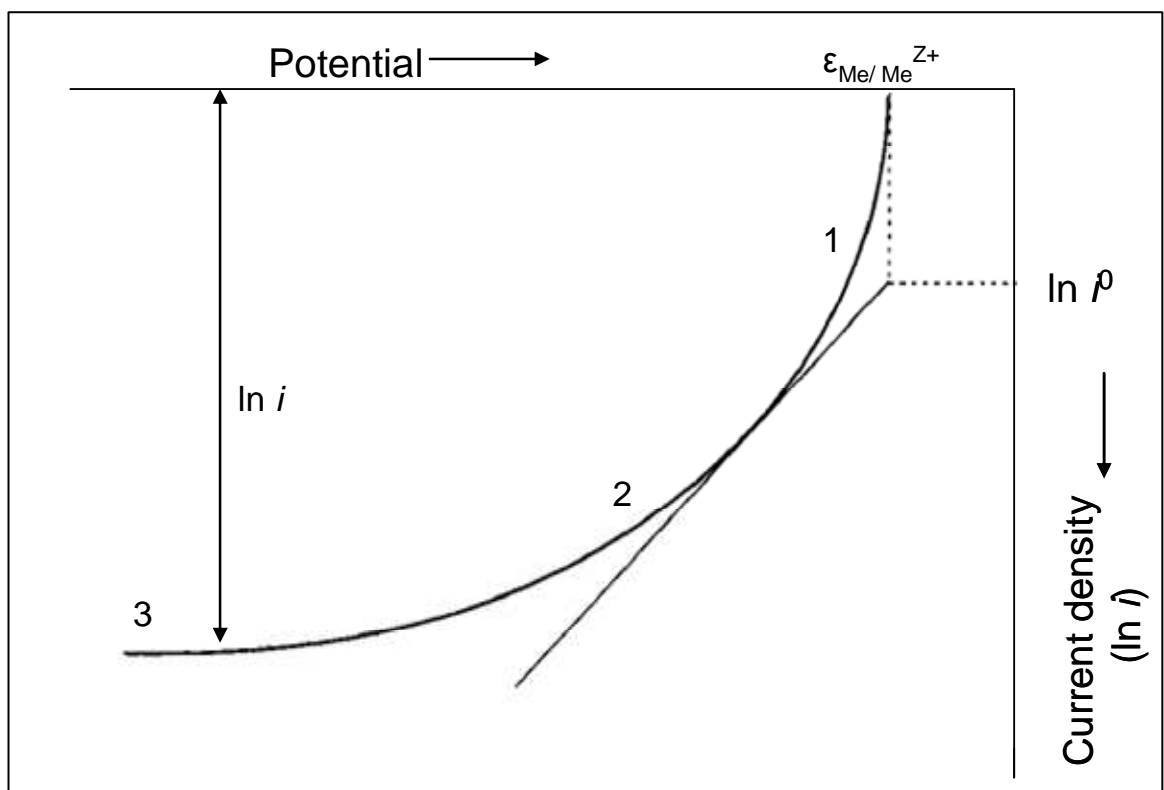


Figure 2.6: Shape of the current-voltage plot: (1) under activation control, (2) intermediate region with both mechanisms rate-determining and (3) under diffusion control

IA	IIA	IIIB	IVB	VB	VIB	VII B	VIII B				IB	IIB	IIIA	IVA	VA	VIA	VIIA	VIIIA
1 H																		2 He
3 Li	4 Be											5 B	6 C	7 N	8 O	9 F	10 Ne	
11 Na	12 Mg											13 Al	14 Si	15 P	16 S	17 Cl	18 Ar	
19 K	20 Ca	21 Sc	22 Ti	23 V	24 Cr	25 Mn	26 Fe	27 Co	28 Ni	29 Cu	30 Zn	31 Ga	32 Ge	33 As	34 Se	35 Br	36 Kr	
37 Rb	38 Sr	39 Y	40 Zr	41 Nb	42 Mo	43 Tc	44 Ru	45 Rh	46 Pd	47 Ag	48 Cd	49 In	50 Sn	51 Sb	52 Te	53 I	54 Xe	
55 Cs	56 Ba	57 La	72 Hf	73 Ta	74 W	75 Re	76 Os	77 Ir	78 Pt	79 Au	80 Hg	81 Tl	82 Pb	83 Bi	84 Po	85 At	86 Rn	
87 Fr	88 Ra	89 Ac	104 Ku															

Figure 2.7: Periodic table showing those metals (inside frame and shaded) which can be deposited from aqueous solution

2.3 Components of plating bath

Hydrogen evolution reaction (HER) often occurs in the aqueous based electrolyte electrodeposition resulting in profound effect on current efficiency and quality of the metal deposited. As a result, different additives may be needed to suppress such difficulties [5]. A wide range of organic molecules such as polyethylene glycol (PEG), polypropylene glycol (PPG), thiourea, gelatin, hydroquinone and etc. are added in relatively low concentration to the electroplating bath to modify the structure, morphology and properties of the deposit. Their involvement has been almost totally empirical and details of their mode of operation are seldom known. Indeed, it is not always clear whether their effect is due to the additive itself or to decomposition products formed in electrode reactions. Several generalizations concerning their operation are, however, possible. Certainly, additives are usually capable of adsorption on the cathode surface, and in some cases organic matter is occluded into the deposit, especially when the plated metal has a high surface energy (high melting point). Many additives also increase the deposition overpotential and change the Tafel slope. This may be due to the need for electron transfer to occur through the adsorbed layer or due

to complex formation at the electrode surface. While the additives may affect more than one property of the deposit and there is clear evidence that when several additives are present in the electrolyte their effect is synergistic, they are often classified in the following [11]:

1. Brighteners- For a deposit to be bright, the microscopic roughness of the deposit must be low compared with the wavelength of the incident light so that is reflected rather than scattered. Brighteners are commonly used in relatively high concentration (several g dm^{-3}) and may result in substantial organic matter in deposit. They usually cause the deposit formed as an even and fine-grained, hence, may act as modifier to the nucleation process.
2. Levelers- These produce a level deposit on a more macroscopic scale and act by adsorption at points where otherwise there would be rapid deposition of metal. Thus, adsorption of additives occurs preferentially at dislocations because of a higher free energy of adsorption and at peaks. The phenomenon happened due to the rate of their diffusion to such points is enhanced, the adsorbed additive will reduce the rate of electron transfer. In practice, additive act as both brighteners and levellers.
3. Structure modifiers- These additives change the structure of the deposit and maybe even the preferred orientation or the type of lattice. Some are used to optimize particular deposit properties, and others to adjust the stress in the deposit (stress is due to lattice misfit). The latter are often called “stress relievers”.

4. Wetting agents- These are added to accelerate the release of hydrogen gas bubbles from the surface. In their absence, the hydrogen which is often evolved in a parallel reaction to metal deposition can become occluded in the deposit causing, for example, hydrogen embrittlement.

2.4 Ionic Liquid

The recognized definition of an ionic liquid is “an ionic material that is liquid below 100 °C” but leaves the significant question as to what constitutes an ionic material. The whole electroplating sector is based on aqueous solutions. Clearly, the key advantages of using aqueous solution are [5]:

1. Cost
2. Non-flammable
3. High solubility of electrolytes
4. High conductivities resulting in low ohmic losses
5. High solubility of metal salts
6. High rate of mass transfer

For these reason, water will remain the mainstay of the metal plating industry. However, there are also limitations of aqueous solutions including [5]:

1. Limited potential windows
2. Gas evolution processes can be technically difficult to handle and result in hydrogen embrittlement.
3. Passivations of metals cause difficulties with both anodic and cathodic materials.
4. Necessity for organic additives.

5. All water must eventually be returned to the water source.

2.4.1 Deposition with Ionic Liquid

In contrast, a fundamental advantage of using ionic liquid electrolytes in electroplating is that, since these are non-aqueous solutions, there is negligible hydrogen evolution during electroplating and the coatings possess the much superior mechanical properties of the pure metal. Hence essentially crack-free, more corrosion-resistant deposits are possible. This may allow thinner deposits to be obtained, thus reducing overall material and power consumption. Between year 1980 and 2000 most of the studies on the electrodeposition in ionic liquids were performed in the first generation of ionic liquids, formerly called “room-temperature molten salts” or “ambient temperature molten salts”. The recognized definition of an ionic liquid is an ionic material that is liquid below 100 °C. A series of transition and main-group metal containing ionic liquids have been formulated and the feasibility of achieving electrodeposition has been demonstrated for the majority of these metals, **Figure 2.8** shows the elements in the periodic table that have been deposited using ionic liquids. It must be stressed that while the deposition of a wide range of metals has been demonstrated from a number of ionic liquids the practical aspects of controlling deposit morphology have not been significantly addressed due to the complex nature of the process parameters that still need to be understood. Despite the lack of reliable models to describe mass transport and material growth in ionic liquids, there are tantalizing advantages that ionic liquid solvents have over aqueous baths that make the understanding of their properties vitally important. Some of these advantages include [5]:

1. Electroplating of a range of metals impossible to deposit in water due to hydrolysis e.g. Al, Ti, Ta, Nb, Mo, W. As an example, the deposition of Al by

electrolysis in a low-temperature process has long been a highly desirable goal, with many potential applications in aerospace for anti-friction properties, as well as replacing Cr in decorative coatings. The deposition of Ti, Ta, Nb, Mo, will open important opportunities in various industries, because of their specific properties (heat, corrosion, abrasion resistance, low or high density etc.).

2. Direct electroplating of metals on water-sensitive substrate materials such as Al, Mg and light alloys with good adherence should be possible using ionic liquids.
3. There is potential for quality coatings to be obtained with ionic liquids rather than with water. Currently available metallic coatings suffer from hydrogen embrittlement; a major problem caused by gaseous hydrogen produced during water electrolysis. During electroplating with ionic liquids, negligible hydrogen is produced, and coatings will have the better mechanical properties.
4. Metal ion electrodeposition potentials are much closer together in ionic liquids compared with water, enabling easier preparation of alloys and the possibility of a much wider range of possible electroplated alloys, which are difficult or impossible in water.
5. Ionic liquids complex metals offer the possibility to develop novel electroless plating baths for coating polymers (e.g. in electronics) without the need for the toxic and problematic organic complexants used in water.
6. Although the cost of ionic liquids will be greater than aqueous electrolytes, high conductivity and better efficiency will provide significant energy savings

compared with water, and capital costs will be much lower than the alternative techniques such as PVD and CVD.

7. When used in electropolishing and electropickling processes, strongly acidic aqueous electrolytes create large quantities of metal-laden, corrosive effluent solution, whereas in ionic liquid electrolytes the metals will precipitate and be readily separated and recycled.
8. The replacement of many hazardous and toxic materials currently used in water, e.g. toxic form of chromium (VI), cyanide, highly corrosive and caustic electrolytes, would save about 10% of the current treatment costs.
9. Nano composite coatings – nano particles giving improved properties compared to micro particles e.g. thermal and electrical conductivity, transparency, uniformity, low friction.
10. An increased range of metal coatings on polymers is accessible by electroless plating using ionic liquids containing reducing agents.


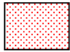
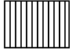
1																	18																												
H	2											13	14	15	16	17	He																												
Li	Be											B	C	N	O	F	Ne																												
Na	Mg	3	4	5	6	7	8	9	10	11	12	Al	Si	P	S	Cl	Ar																												
K	Ca	Sc	Ti	V	Cr	Mn	Fe	Co	Ni	Cu	Zn	Ga	Ge	As	Se	Br	Kr																												
Rb	Sr	Y	Zr	Nb	Mo	Tc	Ru	Rh	Pd	Ag	Cd	In	Sn	Sb	Te	I	Xe																												
Cs	Ba	La	Hf	Ta	W	Re	Os	Ir	Pt	Au	Hg	Tl	Pb	Bi	Po	At	Rn																												
Fr	Ra	Ac																																											
<table border="1"> <tr> <td>Ce</td> <td>Pr</td> <td>Nd</td> <td>Pm</td> <td>Sm</td> <td>Eu</td> <td>Gd</td> <td>Tb</td> <td>Dy</td> <td>Ho</td> <td>Er</td> <td>Tm</td> <td>Yb</td> <td>Lu</td> </tr> <tr> <td>Th</td> <td>Pa</td> <td>U</td> <td>Np</td> <td>Pu</td> <td>Am</td> <td>Cm</td> <td>Bk</td> <td>Cf</td> <td>Es</td> <td>Fm</td> <td>Md</td> <td>No</td> <td>Lr</td> </tr> </table>																		Ce	Pr	Nd	Pm	Sm	Eu	Gd	Tb	Dy	Ho	Er	Tm	Yb	Lu	Th	Pa	U	Np	Pu	Am	Cm	Bk	Cf	Es	Fm	Md	No	Lr
Ce	Pr	Nd	Pm	Sm	Eu	Gd	Tb	Dy	Ho	Er	Tm	Yb	Lu																																
Th	Pa	U	Np	Pu	Am	Cm	Bk	Cf	Es	Fm	Md	No	Lr																																
		As metal																																											
		As alloy																																											
		As Metal and Alloy																																											

Figure 2.8: Summary of the elements deposited as single metal or alloys

2.4.2 Electrodeposition of Tin with Ionic Liquid

Electrodeposition of Sn in ionic liquids was rarely studied in the past. Few studies were reported on the electrodeposition of Tin(II) in ionic liquids. The first was done by Hussey and Xu [7] in an AlCl_3 mixed in 1-methyl-3-ethyl imidazolium chloride melt. W. Yang *et al.* [8] has done Tin and Antimony electrodeposition in 1-ethyl-3-methylimidazolium tetrafluoroborate, and N. Tachikawa *et al.* [9] has done electrodeposition of Tin(II) in a hydrophobic ionic liquid, 1-*n*-butyl-1-methylpyrrolidinium bis(trifluoromethylsulfonyl)imide.

In the work that carried out by Hussey and Xu, the ionic liquid 1-ethyl-3-methylimidazolium chloride $[\text{EMIm}]^+\text{Cl}^-$ that they deployed is also called room temperature molten salts. This is a mixture of aluminum chloride and an organic halide (RX). It shows adjustable Lewis acidity depending on AlCl_3/RX molar ratios [7].

Hussey and Xu showed that the electrodeposition of Sn on platinum in $\text{AlCl}_3\text{-EMIC}$ is a quasi-reversible process [7].

W. Yang *et al.* [8] has done tin and antimony electrodeposition in 1-ethyl-3-methylimidazolium tetrafluoroborate, $[\text{EMIm}]\text{BF}_4$. In W. Yang *et al.* work, the Sn(II) was introduced into the $[\text{EMIm}]\text{BF}_4$ along with SnCl_2 . In the linear sweep voltammetry (LSV) experiments, the cathodic peak potentials of Sn(II) shifted negatively as the potential scan rate increased. This had indicated that the Sn(II) reductions on Pt electrode exhibit electrochemically irreversible behaviors (**Figure 2.9**). The surface morphologies were examined by SEM (**Figure 2.10**). The tin deposit produced was just needle-type islands, not a continuous plating film on Pt surface [8].

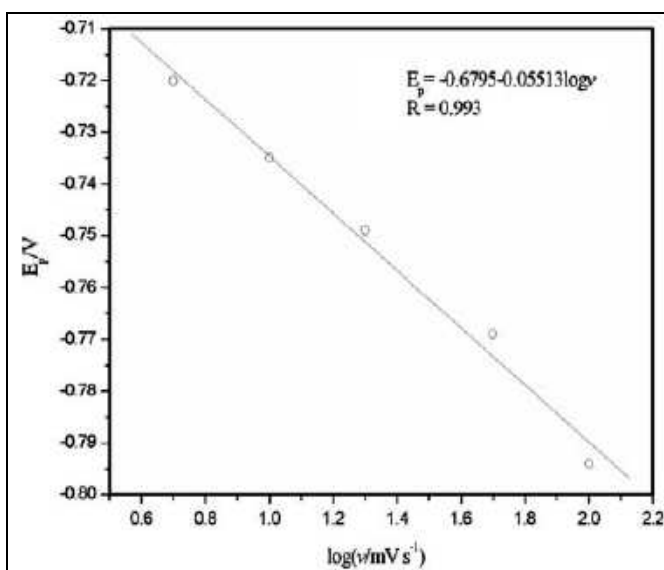


Figure 2.9: Linear relationship between the cathodic peak potential of Sn(II) reduction & the logarithm of potential scan rate in the $[\text{EMIm}]\text{BF}_4$ containing 25 mM Sn(II) [8].

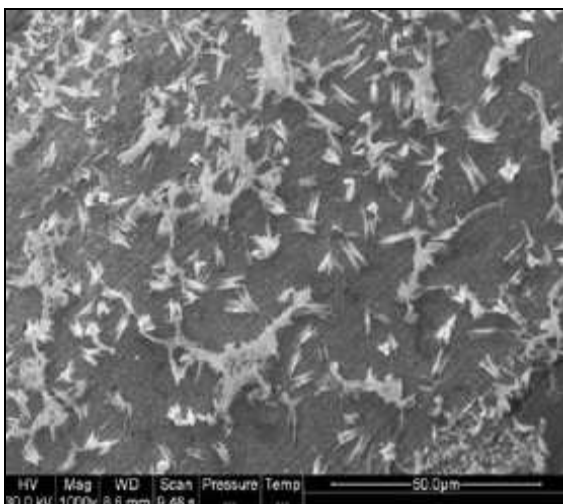


Figure 2.10: SEM micrographs of metal electrodeposits from the [EMIm]BF₄ ionic liquid containing 25 mM Sn(II) [8].

N. Tachikawa *et al.* [9] has done electrodeposition of Tin(II) in a hydrophobic ionic liquid, 1-*n*-butyl-1-methylpyrrolidinium bis(trifluoromethylsulfonyl)imide (BMPTFSI). N. Tachikawa *et al.* has reported that tin was introduced into the ionic liquid through potentiostatic anodic dissolution. The oxidation of Sn(II) to Sn(IV) was not possible within the electrochemical potential window of BMPTFSI [9]. In AlCl₃-EMIC ionic liquids, the oxidation of Sn(II) to Sn(IV) is possible in a basic solution but not in an acidic one, probably because tetravalent species is stabilized by the complex formation with chloride ions in the basic ionic liquid [9]. In cyclic voltammetry experiments that carried out by N. Tachikawa *et al.*, a cathodic current was observed below -0.6 V as shown in **Figure 2.11**. The current loop of the cathodic current during the cathodic and anodic scan is characteristic of a nucleation process, indicating the cathodic current can be attributed to the deposition of Sn. The anodic current peak can be assigned to the stripping of Sn deposited during the preceding cathodic scan [9].

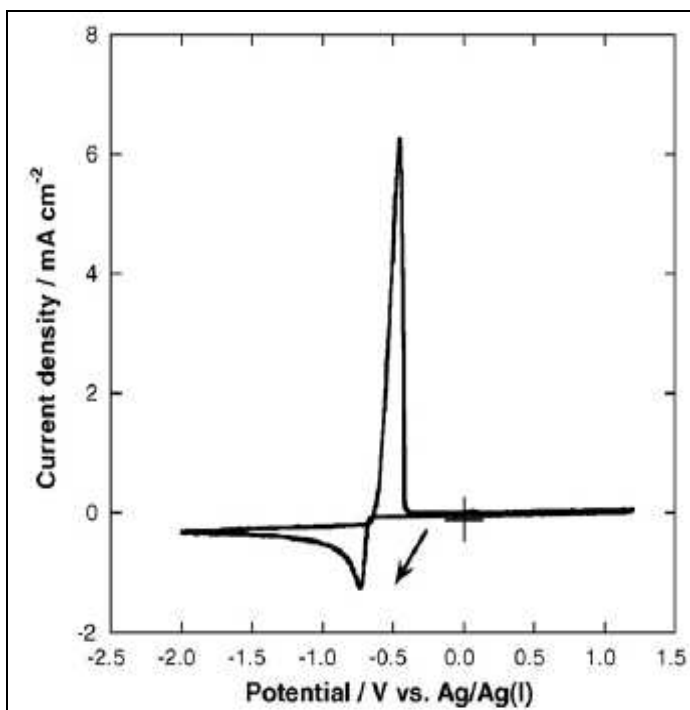


Figure 2.11: Cyclic voltammogram of a Pt electrode in BMPTFSI containing 0.05 mol dm⁻³ Sn(II) at 25 °C; scan rate: 20 mVs⁻¹ [9].

Tachikawa *et al.* has performed the electrodeposition of Sn on a Cu substrate in BMPTFSI containing 0.05 mol dm⁻³ Sn(II) by galvanostatic electrolysis with the current density of -0.05 mA cm⁻². A smooth and adhesive electrodeposit with slight brightness was obtained as shown in **Figure 2.12**.

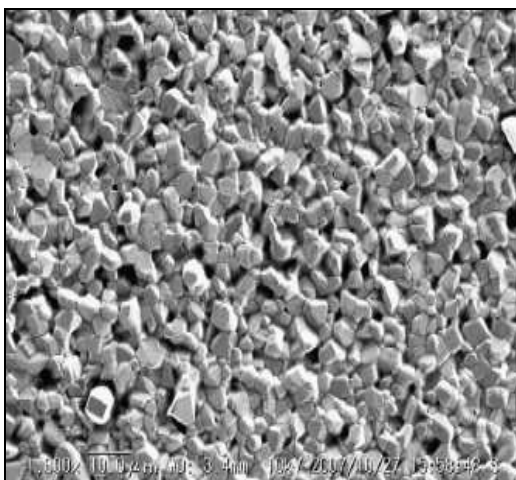


Figure 2.12: SEM image of the deposit on the Cu substrate in BMPTFSI containing 0.05 mol dm⁻³ Sn(II). The current density was -0.05 mA cm⁻² [9].

In 1992, Wilkes and Zaworotko reported the first air and moisture stable imidazolium based ionic liquid with either tetrafluoroborate or hexafluorophosphate as anions. Then, several, liquids consisting of 1-ethyl-3-methylimidazolium, 1,2-dimethyl-3-propylimidazolium, or 1-butyl-1-methyl-pyrrolidinium cations with various anions, such as tetrafluoroborate (BF_4^-), tri-fluoro-methanesulfonate ($CF_3SO_3^-$), bis(trifluoromethanesulfonyl)imide $[(CF_3SO_2)_2N]$ & tris(tri fluoro methanesulfonyl) methide $[(CF_3SO_2)_3C]$, were found and received much attention because of low reactivity against moisture [6]. In view of the advantages of the air and water stable ionic liquids, we report here the first results on the tin electrodeposition via the mixture of ionic liquid and Methane Sulfonic Acid (MSA) based tin methane sulfonate salts.

2.4.3 Electrodeposition of Copper with Ionic Liquid

A study on the electrodeposition of copper in mixture of ionic liquid and acidic electrolyte was reported by Q. B. Zhang *et al.* [18]. Q. B. Zhang *et al.* has carried out copper electrodeposition in an electrolyte which contains mixture of ionic liquid 1-butyl-3-methylimidazolium hydrogen sulfate-[BMIM]HSO₄, sulfuric acid, hydrated copper sulfate and distilled water. [BMIM]HSO₄ is found to be an efficient leveling additive in copper electrodeposition, leading to more leveled and fine grained cathodic deposits. **Figure 2.13** shows the scanning electron micrographs (SEM) of the copper deposition in the absence and in presence of ionic liquid [BMIM]HSO₄ [18].

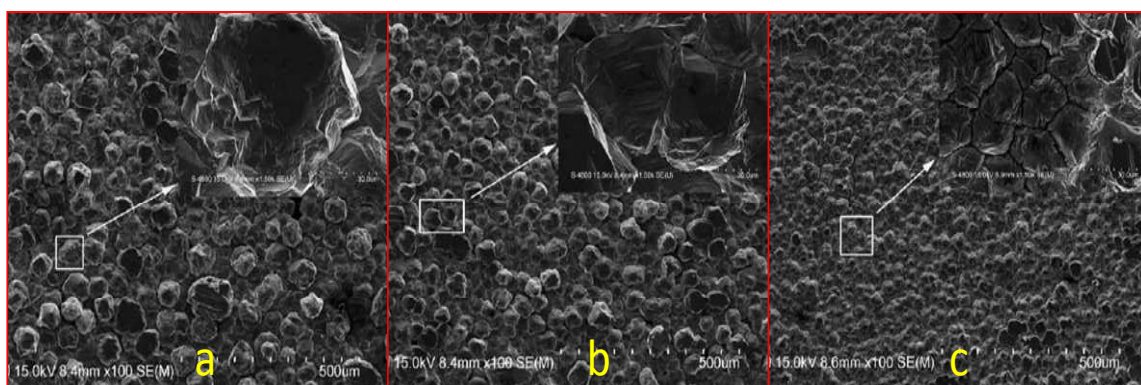


Figure 2.13: SEM of copper deposits in the absence and in presence of [BMIM]HSO₄.

(a) Blank, (b) [BMIM]HSO₄: 10 mg dm⁻³, (c) [BMIM]HSO₄: 50 mg dm⁻³ [18].

The polarization curves obtained from solution without and with different amounts of [BMIM]HSO₄ are shown in **Figure 2.14** [18]. It is clear that the addition of [BMIM]HSO₄ markedly increases the electro-reduction potential of Cu²⁺ ion, along with the reduction of the cathodic current density, denoting an inhibition effect of the electro-crystallization process. [BMIM]HSO₄ increase the cathodic polarization of copper through their adsorption on the cathodic surface and inhibit the kinetics of the Cu²⁺ reduction process [18].

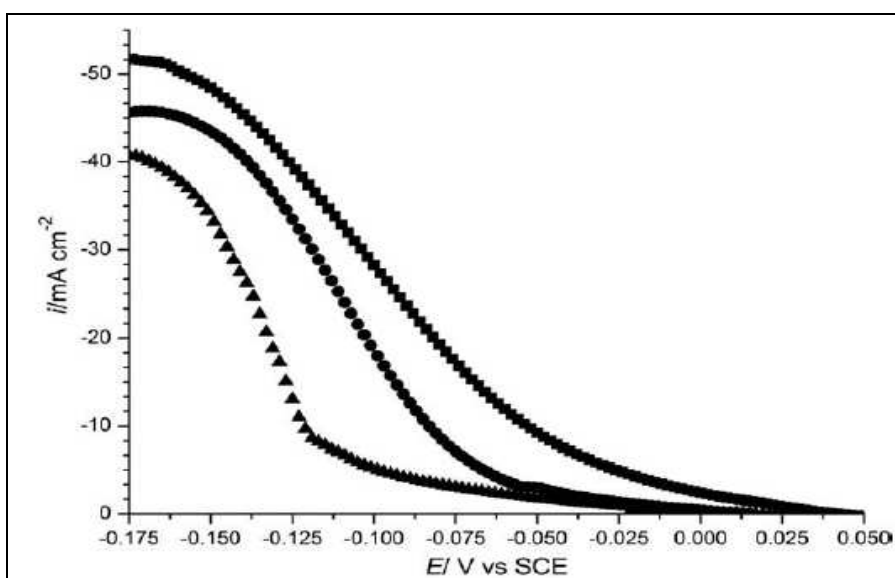


Figure 2.14: Effect of [BMIM]HSO₄ on the cathodic polarization for copper electro-deposition with different concentrations: (■) blank, (●) 10 mg dm⁻³, (▲) 50 mg dm⁻³ [18].

2.4.4 Electrodeposition of Nickel with Ionic Liquid

The electrodeposition behavior of nickel was investigated at glassy carbon and polycrystalline copper electrodes in the 1-ethyl-3-methylimidazolium dicyanamide (EMI-DCA) room-temperature ionic liquid by M. J. Deng *et al.* [4]. Metallic nickel coatings were prepared on copper substrates by potentiostatic reduction of Ni(II). The current efficiency for electrodeposition of Ni from this ionic liquid is higher than 98%. SEM results (**Figure 2.15**) indicated that the morphology of the Ni electrodeposits is dependent on the deposition potential. AFM results (**Figure 2.16**) also showed that the roughness of the nickel-deposited surface increased as the deposition potential decreased [4].

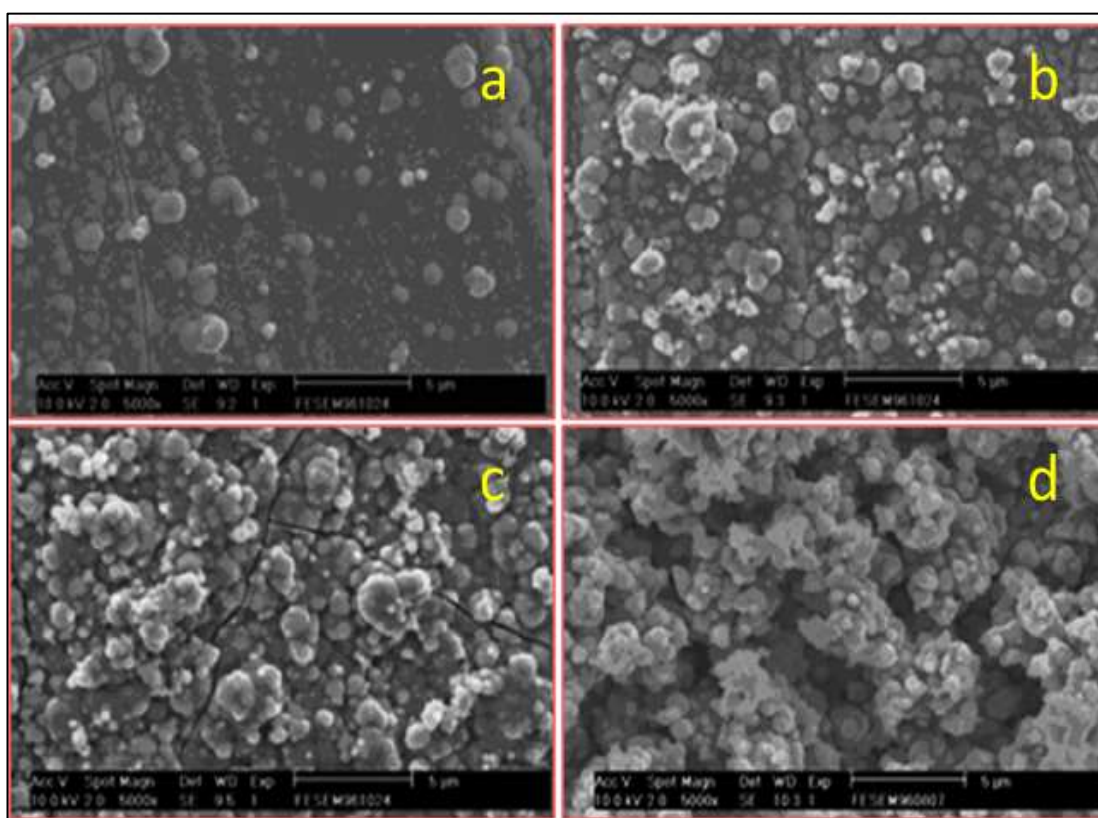


Figure 2.15: SEM micrographs of the nickel electrodeposits in the 0.1 M NiCl₂ EMI-DCA solutions at 301 K. a: -1.4V, b: -1.45V, c: -1.5V, d:-1.6V [4].

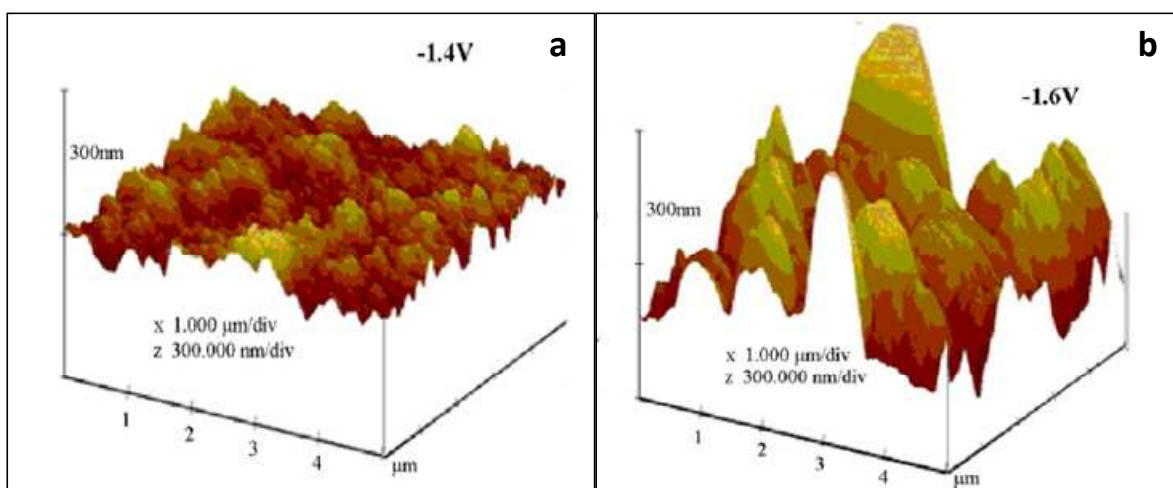


Figure 2.16: AFM micrographs of nickel electrodeposits in the 0.1 M NiCl₂ EMI-DCA solutions at 301 K. a: -1.4 V, b: -1.6 V [4].

2.4.5 Electrodeposition of Cobalt with Ionic Liquid

The electrodeposition of metallic cobalt from a 1-butyl-3-methylimidazolium tetrafluoroborate (BMIMBF₄) ionic liquid was investigated by C. Su *et al.* [19]. The cyclic voltammograms of Co(II) in BMIMBF₄ ionic liquid on a Pt working electrode at different scan rates was recorded. The results showed that the reduction of Co(II) to cobalt on a Pt electrode was an irreversible process and controlled by the diffusion of Co(II). The diffusion coefficient for the reduction of Co(II) was calculated to be 1.76×10^{-8} cm²/s at 60 °C. The cobalt plating was uniform, dense, shining in appearance with good adhesion to the platinum substrate at 60 °C as shown in **Figure 2.17** [19].

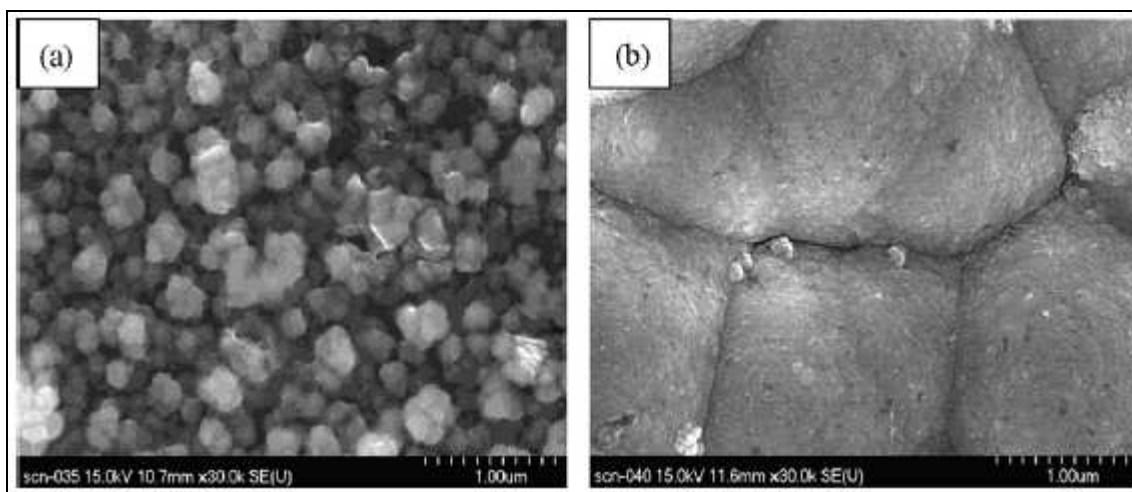


Figure 2.17: SEM of cobalt deposits on platinum wires obtained from a solution of 0.5M Co(II) in BMIMBF₄ ionic liquid at different bath temperatures: (a) 40 °C and (b) 60 °C [19].

2.4.6 Electrodeposition of Aluminum with Ionic Liquid

Few studies were reported on the electrodeposition of aluminum in ionic liquids. In S. Z. E. Abedin *et al.* study [6], it has reported that aluminum is highly reactive ($E^0 = -1.67$ V vs. NHE), the electrodeposition of aluminum in aqueous solutions is impossible owing to a massive hydrogen evolution at the cathode. Therefore, the electrolytes must be aprotic, such as molten salts or organic solvents. The electrodeposition of aluminum in organic solutions had limited success due to a low electrochemical window, low electrical conductivity, volatility, and flammability [6]. Electrodeposition of aluminum and its alloys in ionic liquids based on AlCl₃ was studied intensively in the past. These ionic liquids, formally called room temperature molten salts, are mixtures of aluminum chloride and an organic halide (RX), such as 1-ethyl-3-methylimidazolium chloride [EMIm]⁺Cl⁻. They show adjustable Lewis acidity depending on AlCl₃/RX molar ratios. Liquids with more than 50 mol% AlCl₃ are Lewis acidic; less than 50 mol%, Lewis basic and neutral if the molar ratio AlCl₃/RX is 1 [6].

According to S. Z. E. Abedin *et al.*, a major disadvantage of AlCl_3/RX is that the organic halide and AlCl_3 as educts for the liquid are hygroscopic and extremely hygroscopic, respectively. Therefore, both the educts and the final ionic liquid must strictly be handled under an inert atmosphere or at least under dry air. Furthermore, it is not a standard procedure in the laboratory to make the organic halides water free. Thus, the synthesis of the rather novel air and water stable ionic liquids stimulated further interest in the use of ionic liquids in electrodeposition [6].

S. Z. E. Abedin *et al.* [6] have evaluated ionic liquid 1-butyl-1-methyl pyrrolidinium bis(trifluoromethylsulfonyl)imide saturated with AlCl_3 in their study. AlCl_3 dissolves well and homogeneously in the ionic liquid up to a concentration of about 1.5 mol/L giving a clear solution, from which aluminum cannot be deposited. By further increasing of the concentration of AlCl_3 a biphasic mixture is obtained. By adding more AlCl_3 the volume of the lower phase decreases till reaching a concentration of 2.7 mol/L, then only one solid phase is obtained at room temperature. The biphasic mixture AlCl_3/IL becomes monophasic by heating up to a temperature of 80 °C as shown in **Figure 2.18**.

S. Z. E. Abedin *et al.* have examined the electrodeposition of aluminum from both phases and they have found that at room temperature aluminum can only be deposited from the upper phase. This is believed that the lower phase is formed by neutral, mixed chloro-[bis(trifluoromethansulfonyl)imide]-aluminium species. In contrast, the upper phase contains the organic cation and a mixture of chloro-[bis(trifluoromethansulfonyl)imide]-aluminate ions. This means that reducible aluminum containing species only exist in the upper phase of the AlCl_3/IL mixture and hence the electrodeposition of aluminum occurs only from the upper phase [6].

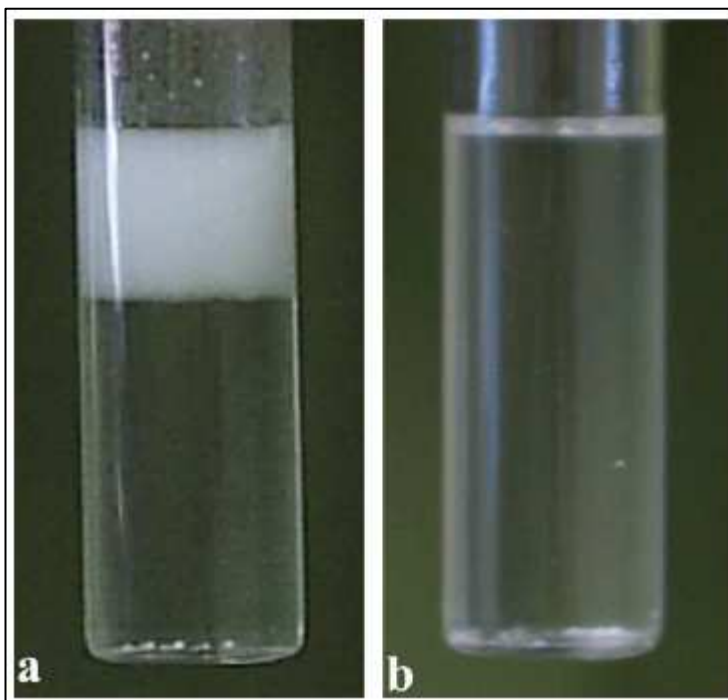


Figure 2.18: (a) A biphasic mixture of the ionic liquid 1-butyl-1-methyl pyrrolidinium bis(trifluoromethylsulfonyl)imide containing 1.6 M AlCl_3 at room temperature. (b) The biphasic mixture becomes monophasic at 80 °C [6].

S. Z. E. Abedin *et al.* have carried out the cyclic voltammetry under two different conditions. One was under room temperature and another one was at 100 °C. A clear nucleation loop is observed in the forward scan for cyclic voltammetry at room temperature as shown in **Figure 2.19**. It indicates that the bulk deposition of aluminum in this complicated system seems to require certain overpotential. However, when the cyclic voltammetry study carried out at 100 °C, in the reverse scan, the anodic scan does not intersect the cathodic one indicating that the deposition of aluminum onto gold substrate at 100 °C does not require an overpotential to initiate nucleation and growth of the bulk deposit (**Figure 2.20**).

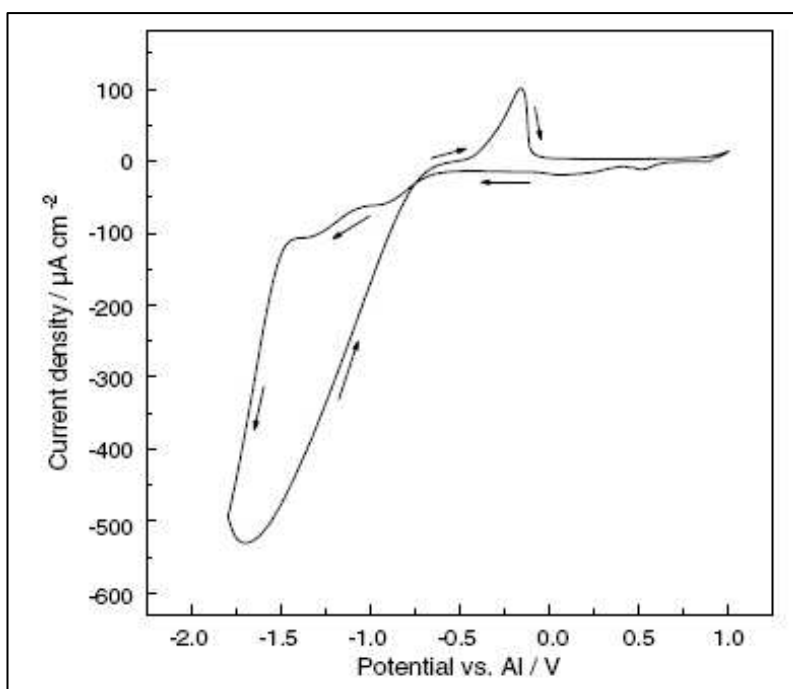


Figure 2.19: Cyclic voltammogram in the ionic liquid ([BMP]-Tf₂N) containing 1.6M AlCl₃ at room temperature [6].

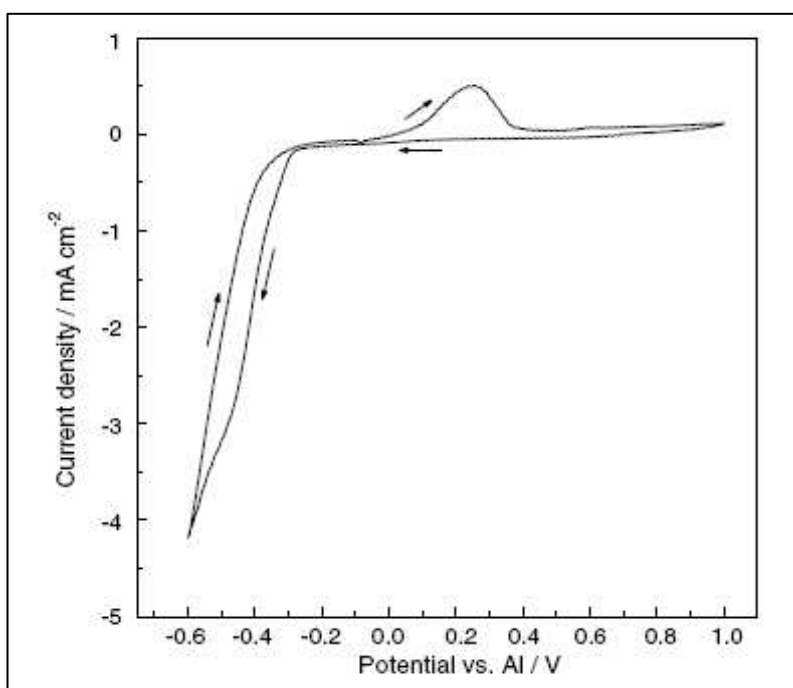


Figure 2.20: Cyclic voltammogram in the ionic liquid ([BMP]-Tf₂N) containing 1.6M AlCl₃ at 100 °C [6].

The aluminum electrodeposits obtained at room temperature and at 100 °C were investigated by means of a high resolution field-emission scanning electron microscope (SEM) by S. Z. E. Abedin *et al.* Based on the SEM diagram (**Figure 2.21**), remarkably the crystallites become finer and deposition improved at 100 °C compared with the study done at room temperature [6].

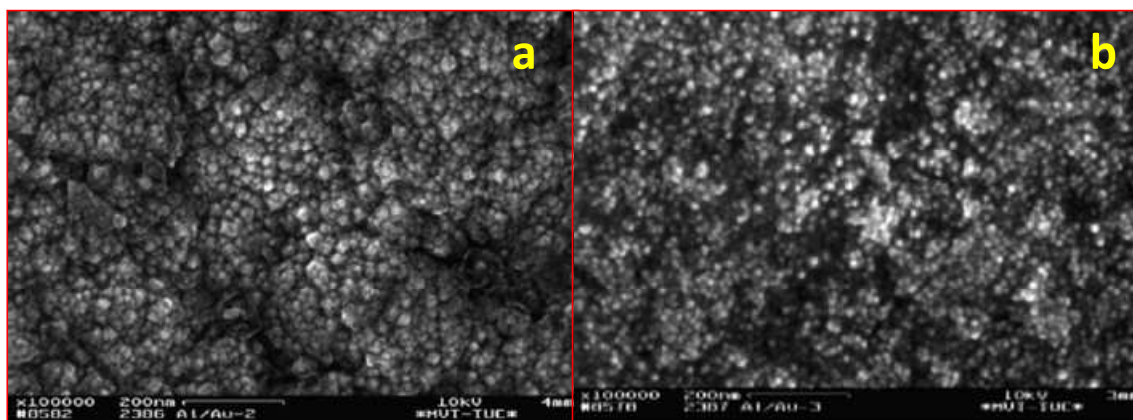


Figure 2.21: SEM micrographs of electrodeposited Al in the upper phase of the mixture AlCl_3 and $[\text{BMP}]\text{Tf}_2\text{N}$: (a) at room temperature; (b) at 100 °C [6].

S. Caporali *et al.* [20] have carried out the electrodeposition of Aluminum in ionic liquid 1-butyl-3-methyl-imidazolium heptachloroaluminate ($[\text{BMIM}]\text{Al}_2\text{Cl}_7$). The aluminum was deposited on carbon steel (UNI Fe360B) as protective coating against steel corrosion.

S. Caporali *et al.* have reported that the current efficiency for the electrochemical reduction of aluminum was nearly 100% in ionic liquid 1-butyl-3-methyl-imidazolium heptachloroaluminate ($[\text{BMIM}]\text{Al}_2\text{Cl}_7$) [20]. The electroreduction process was carried out at constant current density (10 mA cm^{-2}) and controlling the time of deposition. Three series of samples for 1, 2 and 4 hours of deposition were shown in **Figure 2.22**.

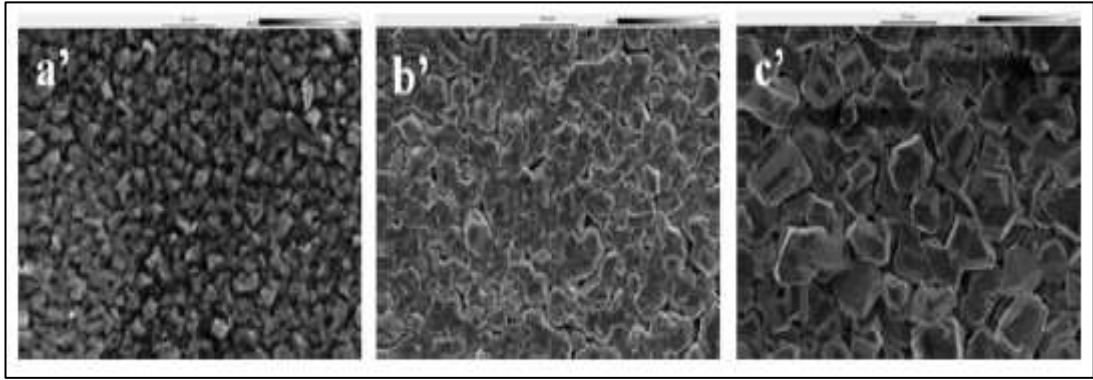


Figure 2.22: SEM micrographs obtained from the carbon steel samples coated with aluminum layers. The samples named a' are obtained after 1 hour deposition, b' after 2 hours and c' after 4 hours [20].

The electrochemical corrosion test on aluminum was studied by S. Caporali *et al.* [20]. Open-circuit potential curves (OCVs) were recorded in aerated 3.5 wt% NaCl aqueous solution as a function of time. In **Figure 2.23** shows the OCV curves obtained for the three different aluminated samples compared with the bare carbon steel and the pure aluminum. The bare carbon steel samples show a shift of the potential towards more negative values reaching the almost constant value of about -0.70 V/SCE after 5 hours. The aluminated samples are characterized by an initial period where the potential remains almost unchanged, followed by a shift towards more negative potentials. This behavior, very close to that of pure aluminum, can be related to the change of the surface due to the degradation of the thin aluminum oxide layer present on the sample and removed in the chloride containing solutions [20].

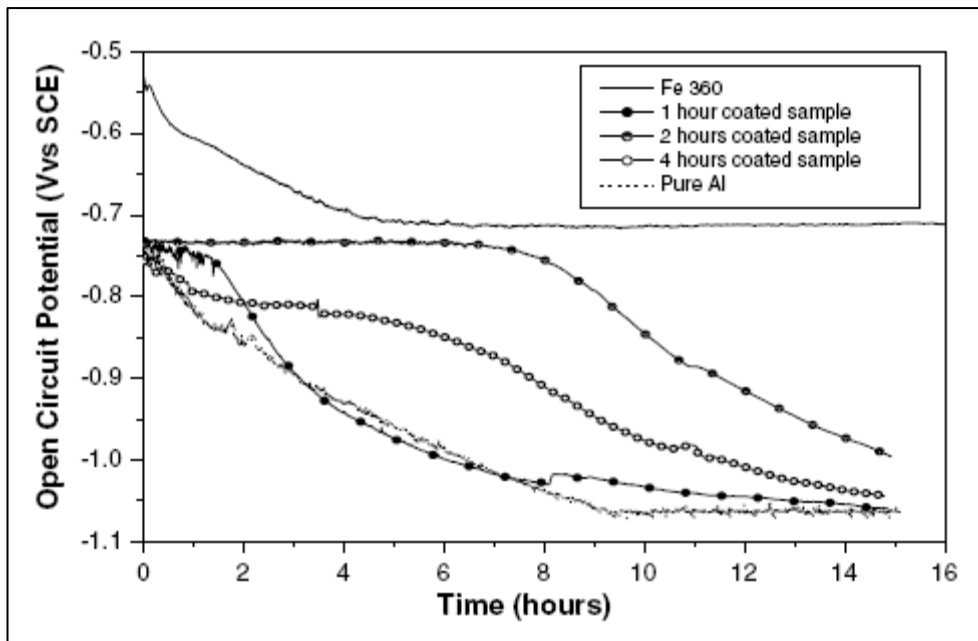


Figure 2.23: OCV curves of different thickness aluminum coated samples compared with the bare carbon steel and the pure aluminum in 3.5 wt% NaCl aqueous solution [20].

Neutral salt spray (NSS) test was also done by S. Caporali *et al.*[20], bare carbon steel and the three series of coated samples with different aluminum thickness, 10 μm , 20 μm and 40 μm were prepared and subjected in the salt spray chamber up to 75 days (**Figure 2.24**).

The evolution of the corrosion spots was the same for all the samples, but the presence of thicker aluminum layer contribute to the slowing down of the corrosion process. After just 1 day, the bare carbon steel samples were completely covered by corrosion. On the other hand, the complete removal of the product with 10 μm coating takes about 30 days (**Figure 2.25**). 20 μm coating take about 70 days of exposition, while at the end of the experiment (75 days) the samples coated with 40 μm of aluminum shown only about the 25% of the coating removed.

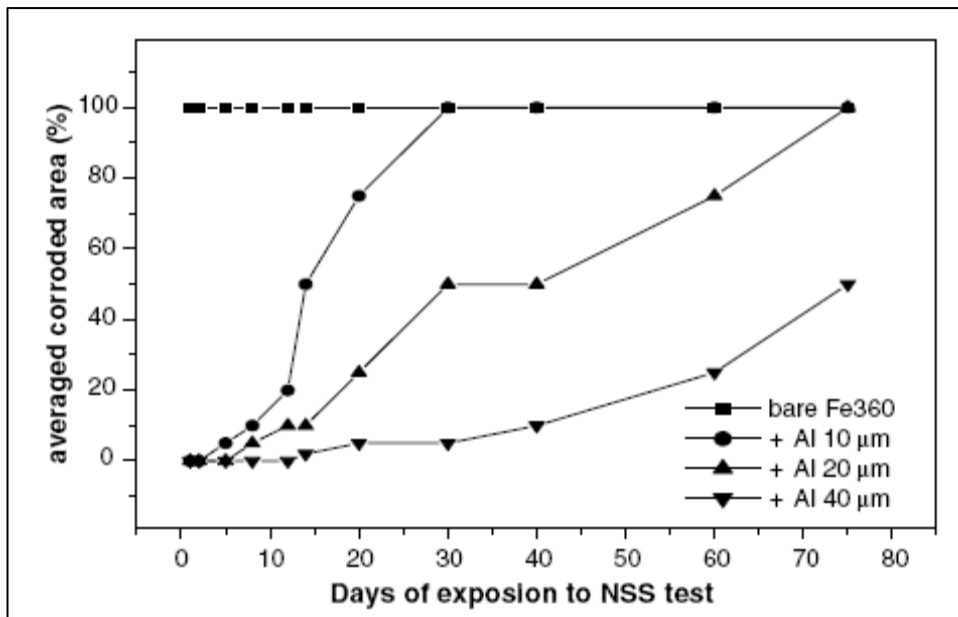


Figure 2.24: Salt spray test corrosion kinetics for the aluminum coated carbon steel [20].

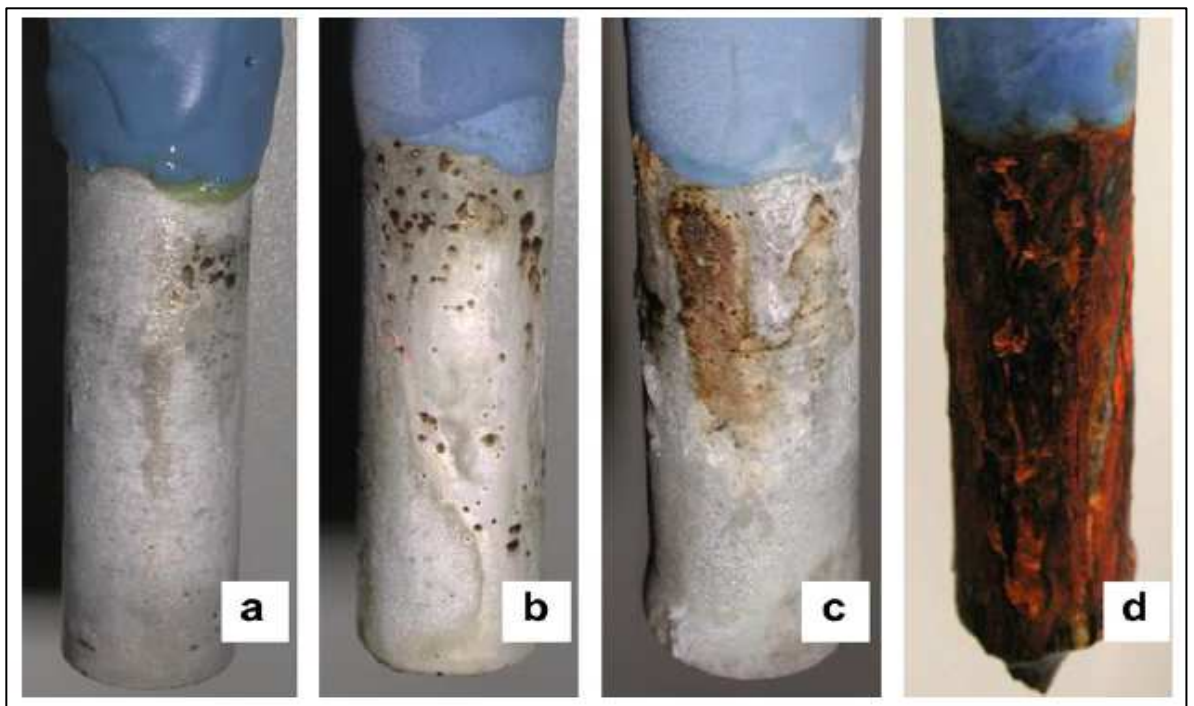


Figure 2.25: Sequence of images showing the process of degradation for a carbon steel sample coated with 10 μm of aluminum during the NSS test. The pictures are taken, respectively, after (a) 5, (b) 8, (c) 14, (d) 30 days of exposure [20].

T. Jiang *et al.* [21] have done the aluminum electrodeposition from acidic AlCl_3 -[EMIm]Cl ionic liquids on aluminum substrates at above room temperatures (60 and 90 °C). The conductivities of 1.5: 1 and 2: 1 AlCl_3 / [EMIm]Cl ionic liquids were measured as a function of the temperature and electrolyte composition. As shown in **Figure 2.26**, the conductivities of ionic liquids increase as the electrolyte temperature increases. This is because the viscosity of the liquid decreases and hence the mobility of the ions increases. The activation energies determined from the slope of the Arrhenius plot (see the inset graph of **Figure 2.26**) are 14.3 kJ/mol for 1.5 :1 AlCl_3 / [EMIm]Cl and 14.6 kJ/mol for 2.0: 1 AlCl_3 / [EMIm]Cl, respectively [21]. In T. Jiang *et al.* study, it was found that 1.5: 1 and 2: 1 AlCl_3 / [EMIm]Cl ionic liquids are quite stable below 100 °C. However, they became dark brown quickly as the temperature increases above 160 °C. The change in the color was probably due to the chemical decomposition of [EMIm]Cl [21].

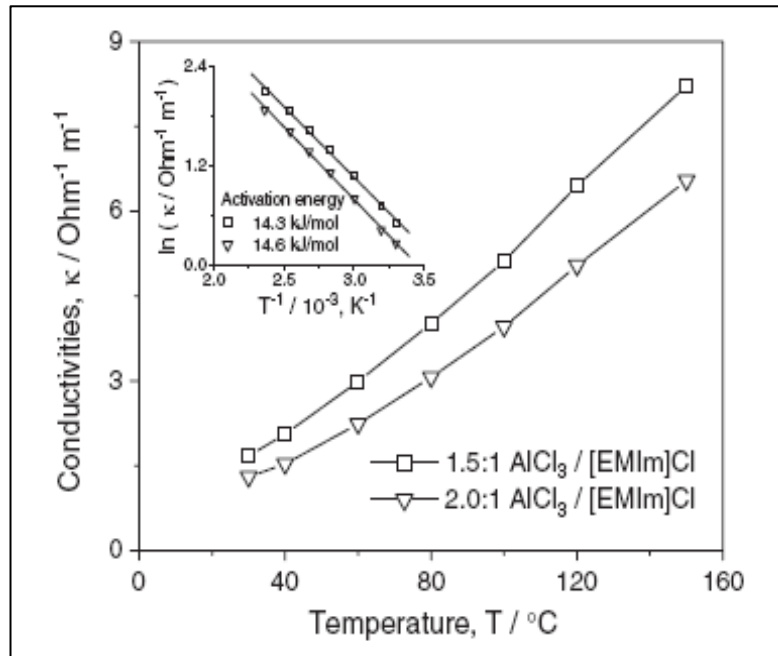


Figure 2.26: Electrical conductivities of AlCl_3 -[EMIm]Cl ionic liquids as a function of the temperature and composition. The inset shows the Arrhenius plot of data [21].

Cyclic voltammetry study was done by T. Jiang *et al.* and the cyclic voltammogram was recorded on aluminum electrode with a scan rate of 100 mV/s (**Figure 2.27**). It is apparent that the cathodic process at C_1 corresponds to the deposition of aluminum whereas the anodic peak at A_1 was ascribed to the subsequent stripping of the deposited aluminum. The anodic oxidation current decreases to almost zero at +0.8 V due to passivation of the Al electrode. It is believed that the passivation behaviors attributed to $AlCl_3$ precipitation on the electrode surface or to the adsorbed monovalent to trivalent aluminum intermediates. However, it is also possible that the decrease of anodic oxidation current is due to the presence of the oxides that were not completely removed from Al electrode by the pre-treatment. Another possibility is the film formation from the decomposition of the organic cation if the deposition is performed at current densities beyond the decomposition limit [21].

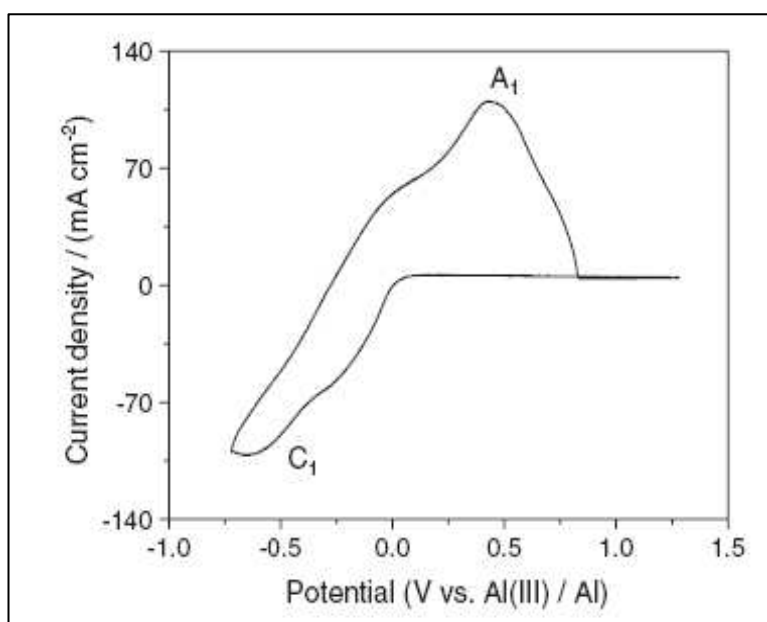


Figure 2.27: A typical voltammogram recorded on Al electrode in 2:1 molar ratio $AlCl_3$ -[EMIm]Cl at 60 °C. Scan rate: 0.1 V/s [21].

The constant current deposition of aluminum from 2: 1 $AlCl_3$ - [EMIm]Cl was carried out on Al substrates by T. Jiang *et al.* **Figure 2.28** shows the surface morphologies of

the four representative aluminum deposits obtained at 20, 30, 50 and 70 mA/ cm². With a current density of 20 mA/ cm², the sample substrate was covered with non continuous aluminum deposits consisting of aluminum crystallites in the order of 30–50 μm in size. The deposits obtained at 30 and 50 mA/ cm² are quite smooth and have similar surface morphology, consisting of aluminum crystalline in the order of 5–10 μm. The deposit obtained at 70 mA/ cm² is much rougher, but it is still quite dense and well adherent. The results also show that the current efficiency increases from 85% to nearly 100% as the current density increases from 10 to 40 mA/ cm². When the current density was raised further, the current efficiency decreases to a constant value of approximately 92% between 50–100 mA/ cm² [21].

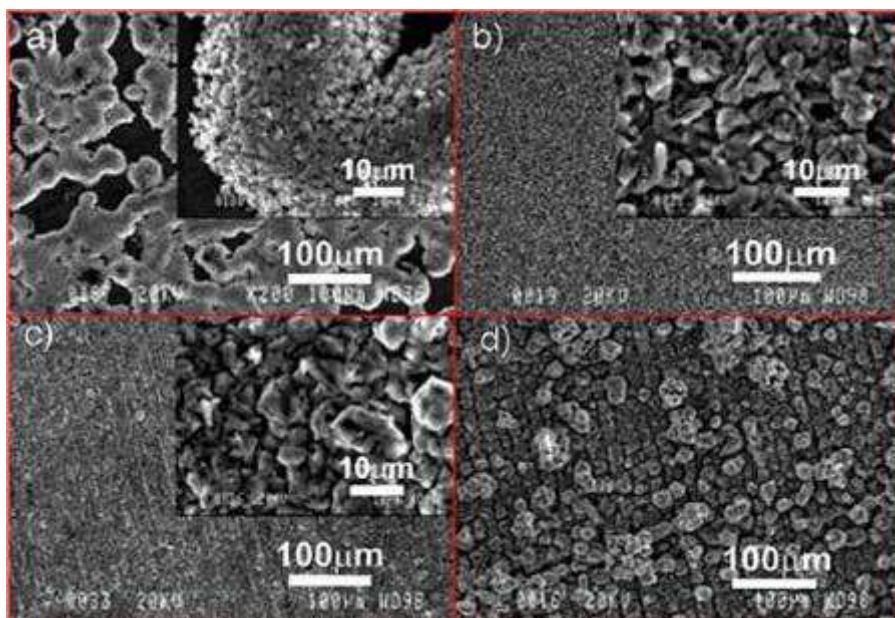


Figure 2.28: SEM micrographs of aluminum electrodeposits obtained on Al substrates from 2:1 molar ratio AlCl₃-[EMIm]Cl at 90 °C with different current densities for 1 hour. a) 20 mA/ cm², b) 30 mA/ cm², c) 50 mA/ cm², d) 70 mA/ cm² [21].

2.4.7 Electrodeposition of Palladium with Ionic Liquid

Y. Bando *et al.* [22] reported that it is not easy to obtain the Pd films without hydrogen embrittlement by electrodeposition from conventional aqueous plating baths since Pd has high catalytic activity against hydrogen evolution and absorbs great amount of hydrogen. As a result, the electrochemical reduction of palladium halide complexes was investigated by Y. Bando *et al.* in a hydrophobic room-temperature ionic liquid (RTIL), 1-n-butyl-1-methylpyrrolidinium bis(trifluoromethylsulfonyl)imide (BMPTFSI) [22]. Cyclic voltammetry experiments was carried out by Y. Bando *et al.*, **Figure 2.29** shows the cyclic voltammogram of the Pt electrode in 10 mM PdCl_4^{2-} /BMPTFSI. The reduction peak of PdCl_4^{2-} appeared at -1.8 V, which was more negative than that for PdBr_4^{2-} by about 0.2 V. The deposition of metallic Pd was also possible from PdCl_4^{2-} /BMPTFSI. The shift in the peak potential can be attributed to the difference in donor property of the ligand. Since the donor number of Cl^- is larger than that of Br^- , the chlorocomplex is expected be more stabilized than the bromocomplex [22].

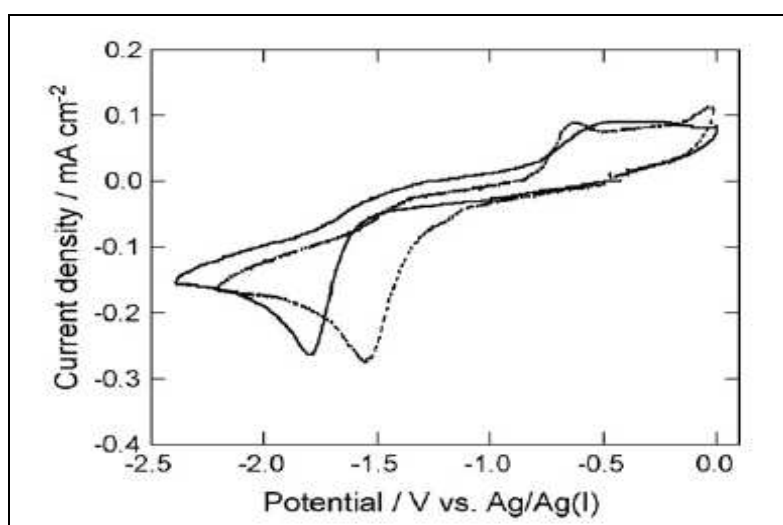


Figure 2.29: Cyclic voltammograms of a Pt electrode in BMPTFSI containing 10 mM PdCl_4^{2-} (—) and 10 mM PdBr_4^{2-} (- - -) at 25 °C. Scan rate: 50mVs⁻¹ [22].

Galvanostatic electrodeposition was carried out by Y. Bando *et al.* and the deposits show at the SEM images (**Figure 2.30**). Black and powdery deposits were obtained at higher current densities (-0.05 mAcm^{-2}). However, smooth deposits with brightness could be obtained at lower current densities (-0.01 mAcm^{-2}). The electrode reaction of PdBr_4^{2-} to metallic Pd was irreversible and the diffusion coefficient of PdBr_4^{2-} was about $(1-2) \times 10^{-7} \text{ cm}^2 \text{ s}^{-1}$ at 25°C . It was suggested by Y. Bando *et al.* that the initial stage of the electrodeposition of Pd from $\text{PdBr}_4^{2-}/\text{BMPTFSI}$ on the polycrystalline Pt electrode surface involves three-dimensional progressive nucleation under diffusion control [22].

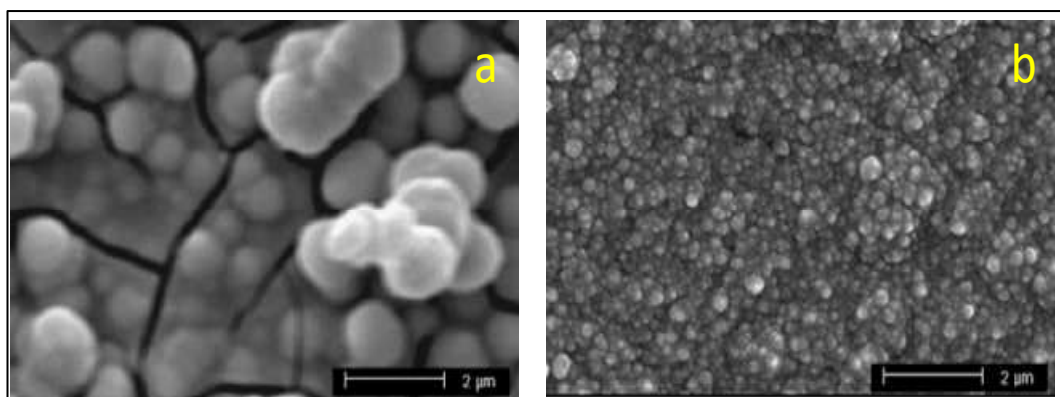


Figure 2.30: SEM images of the deposits on the Ni substrates by the galvanostatic electrodeposition in $10 \text{ mM PdBr}_4^{2-}/\text{BMPTFSI}$ at 25°C . The current densities were (a) -0.05 mAcm^{-2} , (b) -0.01 mAcm^{-2} [22].